Designs of multi-spacecraft swarms for the deflection of Apophis by solar sublimation

Christie Alisa Maddock(1), Massimiliano Vasile(1), Colin McInnes(2), Gianmarco Radice(1), Leopold Summerer(3)

(1)Department of Aerospace Engineering, University of Glasgow
James Watt Building South, University Avenue, Glasgow, United Kingdom, G12 8QQ
Email: c.maddock@aero.gla.ac.uk, m.vasile@aero.gla.ac.uk, g.radice@aero.gla.ac.uk

(2)Department of Mechanical Engineering, Strathclyde University
James Weir Building, 75 Montrose Street, Glasgow, United Kingdom, G1 1XJ
Email: colin.mcinnes@strath.ac.uk

(3)Advanced Concepts Team, European Space Agency (ESA/ESTEC)
Keplerlaan 1, Postbus 299, 2200 AG, Noordwijk, The Netherlands
Email: leopold.summerer@esa.int

Abstract

This paper presents two conceptual designs of multi-spacecraft swarms used for deflecting Apophis. Each spacecraft is equipped with a solar concentrator assembly, which focuses the solar light, and a beaming system that projects a beam of light onto the surface of the asteroid. When the beams from each spacecraft are superimposed, the temperature on the surface is enough to sublimate the rock, creating a debris plume with enough force to slowly alter the orbit of Apophis. An overview of the dynamics, control and navigation strategies are presented along with preliminary system budgets.

INTRODUCTION

In 1993, Melosh [1] proposed the use of a mirror (or solar concentrator) to focus the solar energy onto a small portion of the surface of an asteroid. The resulting heat would sublimate the surface material creating a jet of gas and dust that would produce a continuous thrust. Melosh was proposing the use of a substantially large structure in space, i.e. a primary mirror of 1 km to 10 km in diameter. In a more recent study, Kahle et al. [2] pointed out a number of technological limits of the solar collector idea proposed by Melosh. In particular, the difficulty to operate the mirror in close proximity to the asteroid under the effect of an irregular gravity field and the expected contamination of the primary mirror, due to the ejected gasses. The difficulty of proximal motion control is also shared by another popular method, the gravity tractor. Further disadvantages of the solar collector are the deployment of a large mirror in space, the control of the solar pressure acting on the primary and the power heating up the secondary directional mirror (even assuming a reflectivity of 99% and no contamination).

In 2006, the authors performed a thorough comparison of a number of deflection methods proposed in literature: nuclear explosion, low-thrust tug, gravity tractor, solar sublimation, kinetic impact, and mass driver. Rather than using only one of the comparison criteria used by previous authors, the comparison was based on a multi-criteria approach. Miss distance at the Earth, warning time (time between launch and expected impact with the Earth), mass into space were simultaneously used to assess the optimality of a particular method. Furthermore, rather than using purely hypothetical scenarios or simple theoretical considerations, a wide range of real launch opportunities for each method, and for different classes of asteroids, over a period of 20 years were used to characterise the optimality of a particular method. In order to take into account real mission opportunities and the three criteria at the same time, the concept of set dominance was introduced [3]: given a pair of deflection methods A and B, method A dominates method B if the number of mission opportunities of A that are dominating the mission opportunities of B is higher than the number of mission opportunity of B dominating the mission opportunities of A. Where a mission is dominant over another mission if all the three criteria are better. In other words, a method was better than another if there were more mission opportunities with a better value for all the three criteria. On top of this, a technology readiness level (TRL) factor was applied to all the missions delaying the warning time to account for the required effort to bring the current technology to TRL 9. Note that some methods were excluded from the comparison since the beginning because they require an excessively long warning time (for example, methods based on the Yarkovsky effect). Other methods instead were considered as heavier counterpart of the ones included in the comparison (for example, surface ablation with a laser powered with a nuclear reactor is a heavier counterpart of solar sublimation). The methodology used to model and compare the deflection methods has busted some myths. For example: kinetic impact methods are not always better than low-thrust tugs, though from a theoretical point of view it may appear so. In fact the direction of the impact is rarely optimal while the thrust direction of low-thrust tugs can be steered quite efficiently. Gravity tractors are not insensitive to the morphology of the asteroid because hovering at a distance requires knowledge of the mass distribution of the asteroid. From the comparison the conclusion was that nuclear stand-off explosions were the most effective on the widest range of asteroids. The second best was solar sublimation with all the other methods several orders of magnitude less effective (according to the proposed comparison criteria). Although nuclear explosions were the most effective, a subsequent study by the authors [4] demonstrated that for high level of deflection energy, the risk of a catastrophic fragmentation of the asteroid is not negligible and the total damage caused by a fragmented asteroid is greater than the expected damage caused by the unfragmented asteroid. For lower levels of energy the asteroids either does not fragment catastrophically or re-aggregate after fragmentation due to gravity forces. Due to the possible catastrophic outcome of the nuclear option, the solar sublimation method appeared to be the most interesting deflection method. The problem related to its implementation can be solved if instead of a single mirror, multiple mirrors are used. The idea is to use multiple mirrors of smaller dimensions and to superimpose all the beams of focused light onto the same spot. If the light of the Sun is directly focused on the surface of the asteroid (direct imaging) each spacecraft would be conceptually similar to the one proposed by Melosh. On the other hand, the collected light can be used to pump a laser, which is then used to sublimate the surface.

In this paper, we will analyze both concepts: solar pumped laser and direct imaging. The former concept employs a parabolic reflector which feeds into a solar-pumped laser. A secondary mirror directs the beam to the determined position on Apophis. The orbits are designed to fly in formation with the asteroid around the Sun, and are optimized to minimize the spacecraft-asteroid range and avoid the debris plume. The latter concept places the spacecraft at floating artificial equilibrium points around Apophis, balancing the gravitational effects of the Apophis and the Sun with that of the solar radiation pressure on the spacecraft. The mirror focuses the light directly onto the asteroid surface, controlling the beam by adjusting the shape of the mirror surface. The main advantages of a multi-mirror system are that each spacecraft is relatively small and more easily controllable, the solar pressure on each satellite is reduced and the total power on the secondary mirror is limited. The system is intrinsically redundant: each spacecraft does not represent a single point failure and the system is scalable, all the satellites are identical, therefore a larger asteroid would require simply more satellites without the need for a new design and development. The paper also presents a preliminary analysis of a navigation strategy to simultaneously determine the orbit of the asteroid and to point all the beams onto the same spot on its surface. Finally an initial system budget is estimated for both concepts.

CONCEPTUAL BEE DESIGN

Fig. 1 shows a number of conceptual designs for the focusing system. The designs can essentially be grouped into two categories. For the reflector, either a fixed parabolic or an adaptable mirror can be used. For the focusing system, the only feasible option at present is a solar pumped laser, either directly or indirectly fed. In this paper, the adaptable mirror (Fig. 1a) using direct imaging, and a tri-mirror system with solar pumped laser (Fig. 1b) will be analysed. The configuration in Fig. 1c is not presented in this paper though it was assessed and found more massive in size.

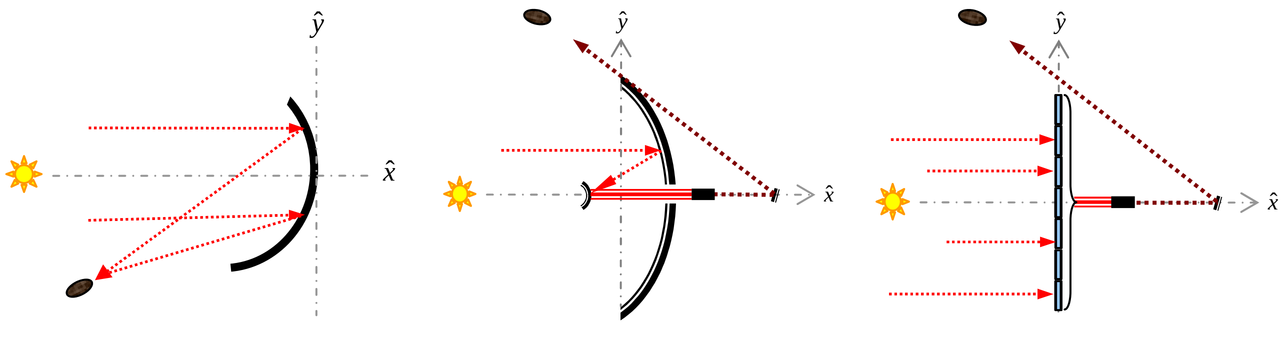

(a) Direct imaging using an adjustable reflector

(b) Dual reflector system with a solar-fed laser followed by a steerable mirror

(c) Solar array for an indirect pumped laser system.

Fig. 1. Conceptual designs for focusing and beaming subsystem

ASTEROID DEFLECTION MODEL

The minimum orbital intersection distance (MOID) is defined as the separation distance at the closest point between two orbits, e.g. Apophis and the Earth. The deviation distance is defined here as the difference in r_A between the original, undeviated orbit and the deviated orbit at t_{moid} [5]. Non-linear equations were derived for determining the difference in r_A are expressed as a function of the ephemeris in the Hill reference frame centred on the asteroid, with $[\Delta i, \Delta\Omega, \Delta\omega, \Delta\theta]$ giving the difference in Keplerian angular parameters between the undeviated and deviated orbit [6].

$$\Delta r = \begin{bmatrix} \rho\cos\theta + \zeta\sin\theta \\ -\zeta\cos\theta + \rho\sin\theta \\ -\cos(\theta-\Delta\theta)\sin\Delta\Omega\sin i + \varpi\sin(\theta-\Delta\theta) \end{bmatrix} \tag{1}$$

where

$$\begin{aligned} \rho &= -\cos\Delta\Omega\cos(\Delta\theta-\theta) + \cos(\Delta i - i)\sin\Delta\Omega\sin(\Delta\theta-\theta) \\ \varpi &= \cos i\sin(\Delta i - i) + \cos\Delta\Omega\cos(\Delta i - i)\sin i \\ \zeta &= \cos i\cos(\Delta\theta-\theta)\sin\Delta\Omega + \left(\cos\Delta\Omega\cos(\Delta i - i)\cos i - \sin(\Delta i - i)\sin i\right)\sin(\Delta\theta-\theta) \end{aligned}$$

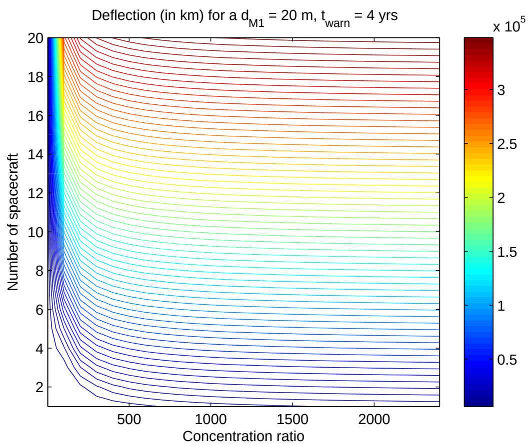

Fig. 2. Deflection as a function of the number of satellites and concentration factor per satellite: laser system operating at 20% efficiency, mirror diameter is 20 m.

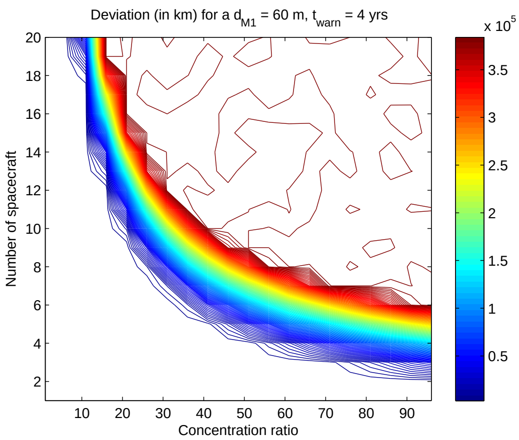

Fig. 3. Deflection as a function of the number of satellites and of the concentration factor per satellite: direct imaging system, mirror diameter is 60 m.

The change in the orbital parameters are calculated by numerically integrating the Gauss planetary equations using a tangential thrust vector $\mathbf{u}_{dev}$ induced by the sublimation method. The change in angular location, in this case given by the mean anomaly, is calculated at the MOID by [5],

$$\Delta M = \int_{t_0}^{t_i} \frac{dM}{dt} dt + n_{A_0}\left(t_0 - t_{moid}\right) + n_{A_i}\left(t_{moid} - t_i\right) \tag{2}$$

where n is the mean motion. The thrust produced by the deflection method is a direct function of the rate of the expelled surface matter [3],

$$\dot{m}_{exp} = 2v_{rot}\iint_{y,t} \frac{1}{E_v}\left(P_{in} - Q_{rad} - Q_{cond}\sqrt{\frac{1}{t}}\right) dt\, dy \longrightarrow \mathbf{u}_{dev} = \frac{\frac{2}{\pi}\bar{v}\,\dot{m}_{exp}}{m_A} \tag{3}$$

where $[t_{in}, t_{out}]$ is the duration for which the point is illuminated, $[y_0, y_{max}]$ are the limits of the vertical component of the illuminated surface area, E_v is the enthalpy of sublimation, P_{in} is the input power due to the solar concentrators, Q_{rad} is the heat loss due to black-body radiation and Q_{cond} is the conduction loss. The magnitude of the induced acceleration $\mathbf{u}_{dev}$ can then determined, where $(2/\pi)$ is the scattering factor assuming the debris plume is uniformly distributed over a half-sphere, $\bar{v}$ is the average velocity of the debris particles according to Maxwell's distribution of an ideal gas, and the remaining mass of the asteroid m_{Ai} is calculated by numerically integrating (3). Fig. 2 shows the deflection that can be achieved with a mirror pumping a laser system with an overall efficiency of 20%, i.e. a laser with an efficiency of 70% and a solar array with an efficiency of about 30%. The concentration factor is the ratio between the cross sectional area of the mirror and the area of the illuminated spot. Fig. 3, instead, shows the deflection that can be achieved by directly projecting the light of the Sun onto the surface of the asteroid. In both cases the deflection operations start 4 years before the first expected impact with the Earth on 13 April 2036.

PROXIMAL MOTION DYNAMICS AND CONTROL

Artificial equilibrium points

If solar pressure and the gravity field of the asteroid are taken into account, then the mirrors can be designed so that the two forces are in equilibrium, with the spacecraft hovering at a given distance from the asteroid, and modifying the shape of the mirror to control the beam. If we consider the gravity field of an asteroid with an ellipsoidal shape, the following set of equations has to be satisfied [7]:

$$\begin{aligned}
&2\dot{v}\left(-y\frac{\dot{r}_A}{r_A}\right)+x\dot{v}^2+\frac{\mu_\odot}{r_A^{\,2}}-\frac{\mu_\odot}{r_s^{\,3}}\left(r_A+x\right)-\frac{\mu_A}{\delta r^3}x+\frac{F_{SRP_x}}{m_s}+\frac{\partial U_{20+22}}{\partial x}=0\\
&-2\dot{v}\left(-x\frac{\dot{r}_A}{r_A}\right)+y\dot{v}^2-\frac{\mu_\odot}{r_s^{\,3}}y-\frac{\mu_A}{\delta r^3}y+\frac{F_{SRP_y}}{m_s}+\frac{\partial U_{20+22}}{\partial y}=0\\
&-\frac{\mu_\odot}{r_s^{\,3}}z-\frac{\mu_A}{\delta r^3}z+\frac{F_{SRP_z}}{m_s}+\frac{\partial U_{20+22}}{\partial z}=0
\end{aligned} \tag{4}$$

where $\mathbf{F}_{SRP}$ is the force acting on the mirror due to solar pressure and U_{20+22} is the gravity of the asteroid. Fig. 4 shows, for different surface areas of the mirror, the points around the asteroid where system (4) is satisfied when the asteroid is at its perihelion. Fig. 5 instead shows the position of the equilibrium points at different positions along the orbit. As it can be seen the position of the equilibrium points is changing due to the rotation of the asteroid (the gravity field changes) and due to distance from the Sun (the solar pressure changes). Note that, though the radial distance changes significantly the ratio between the *x* and the *y* coordinates remains nearly constant, therefore the spacecraft sees the asteroid from the same angle. Fig. 7 show the control needed to keep the spacecraft moving back and forth along the radial direction, 'chasing' the position of the equilibrium points in the case where the spacecraft is in *x*-*y* plane. Equilibrium points with similar characteristics can also be found out of the *x*-*y* plane. Fig. 6 shows a possible strategy to place the spacecraft out of the debris plume in the three dimensional space.

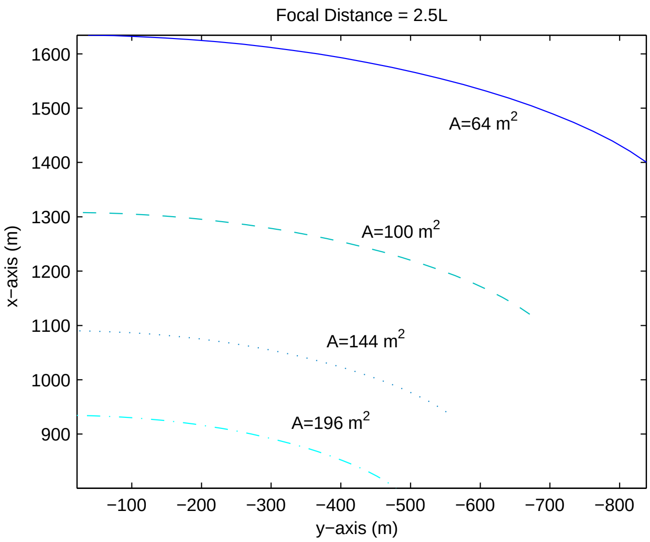

Fig. 4. Artificial equilibrium points for different mirror sizes.

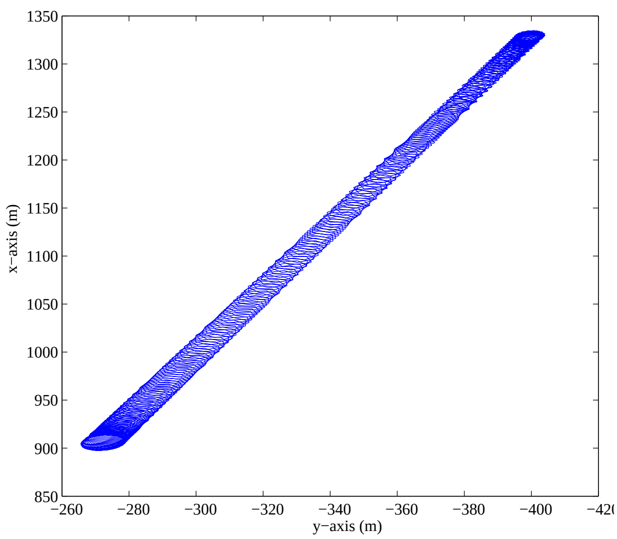

Fig. 5. Variation of AEP over a full orbit of Apophis.

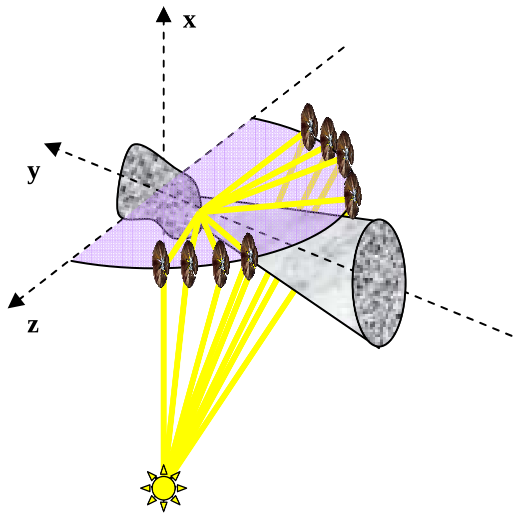

Fig. 6. Strategy to place the mirror in proximity to the asteroid.

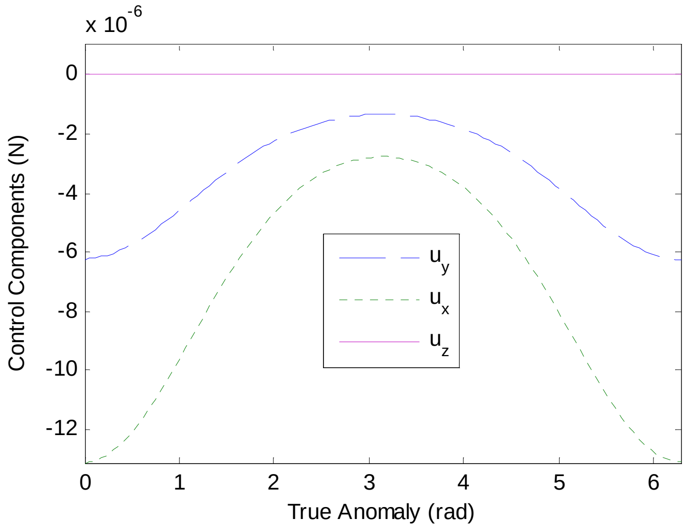

Fig. 7. Control required to follow an AEP using a non-spherical asteroid model.

Funnel orbits

An alternate approach is to have the mirrors flying in formation with the asteroid, orbiting in tandem around the Sun. The formation orbit can be thought of as an orbit around the Sun with a small offset in the initial position and velocity. This offset $[\delta\mathbf{r} \quad \delta\mathbf{v}]$ can be expressed as the difference in the orbital parameters of Apophis and a spacecraft in the formation, given by $\delta\mathbf{k} = [\delta a \quad \delta e \quad \delta i \quad \delta\Omega \quad \delta\omega \quad \delta M]$. The two orbits (i.e. Apophis and the spacecraft) will remain periodic as long as there is no difference in semi-major axes ($\delta a = 0$). As the mean anomaly is a function of the semi-major axis, the difference in mean anomaly will also remain constant throughout the orbit. Schaub and Junkins [8] developed a linear mapping between Hill frame coordinates, and orbit element differences. The linear mapping is an approximation of (1) and holds true so long as $\mathbf{r}_{\odot/A} \gg \delta\mathbf{r}$. The values $\delta\mathbf{k}$ can be optimised to minimise the distance from the asteroid and avoid the plume of gas and debris that is expected to flow along the *y* axis [9]. If that is done, it is possible to identify families of orbits, here called funnel orbits for the configuration that can be seen in Fig. 8.

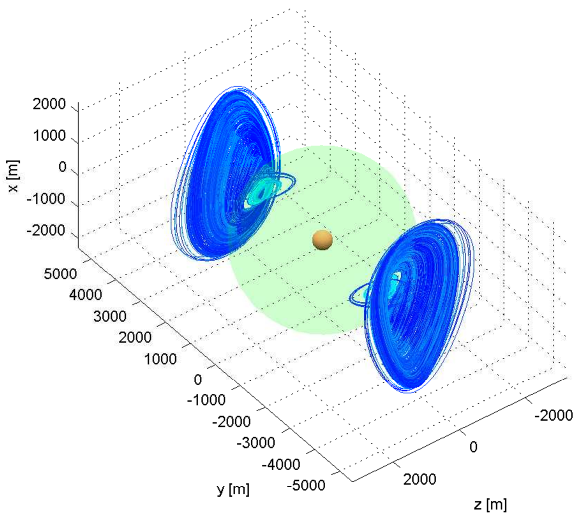

Fig. 8. Set of Pareto-optimal funnel orbits.

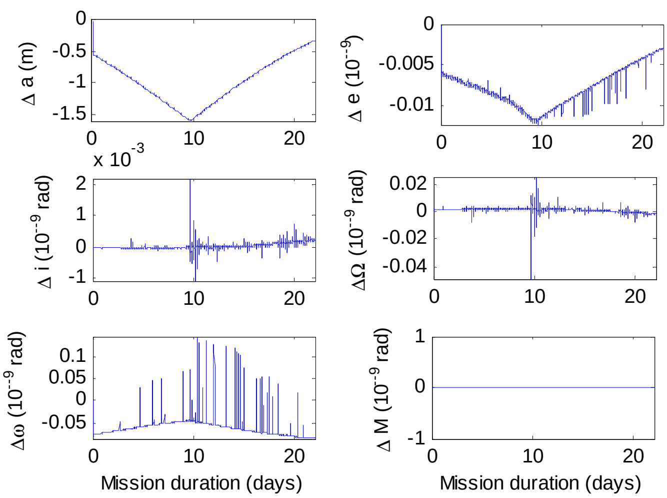

Fig. 9. Variation in $\delta\mathbf{k}$ elements using a feedback control law.

If the inhomogeneous gravity of the asteroid is considered together with solar pressure and with the variation in the orbit of the asteroid due to the deviation, then the funnel orbits need to be controlled to maintain the relative position with respect to Apophis. Fig. 9 shows the variation of the orbital elements obtained with a feedback control law with a thrust magnitude of 0.05 mN.

NAVIGATION

A number of systems, such as the control law, require knowledge of the position and velocity of the asteroid relative to the spacecraft in the formation. It is assumed that the inertial position and velocity of each spacecraft are known from ground measurements. Furthermore, it is assumed that each spacecraft can measure its attitude with a star tracker. In order to determine the location of the asteroid, an onboard camera is used to first determine the angular direction of the asteroid. Using the formation, the range can than be determined by triangulation. With the same technique we can coordinate the steering of all the beams in order to hit the same spot on the surface of the asteroid. The navigation strategy has two goals: to coordinate the pointing control of all the spacecraft in order to intersect the beams and hit the same spot on the surface of the asteroid, and to estimate the position of the asteroid during the deflection manoeuvre. The navigation strategy consists of two steps: first the asteroid is acquired by the camera of a designated leading spacecraft. Once the asteroid is in view of the camera, the camera aligns the centroid of the image of the asteroid with the boresight of the camera (i.e. the origin (0,0) on the camera image plane). The second step is the intersection of the beams and the triangulation of the position of the asteroid. If each camera is aligns the centre of the image plane on the estimated centre of the asteroid, then all the cameras should be pointing along the spacecraft-asteroid vector. Logically then, the intersection point(s) of these beams will create the spot area. For this simulation, the centre of the NEO was used. The spacecraft-asteroid vector (i.e. from the camera to the centre of the NEO) can be written in parametric form,

$$\left[x = w_x t + x_0 \quad y = w_y t + y_0 \quad z = w_z t + z_0 \right] \tag{5}$$

measured in the inertial reference frame. From a simulation point of view, with the angles determined, the only remaining factors to solve are t_1 and t_2 (corresponding to two spacecraft). This can be solved by a minimization function where t is the free variable. Fixing the direction of camera pointing vector, the intersection point is moved until the second camera vector is aligned with the estimated centre of the asteroid from second spacecraft.

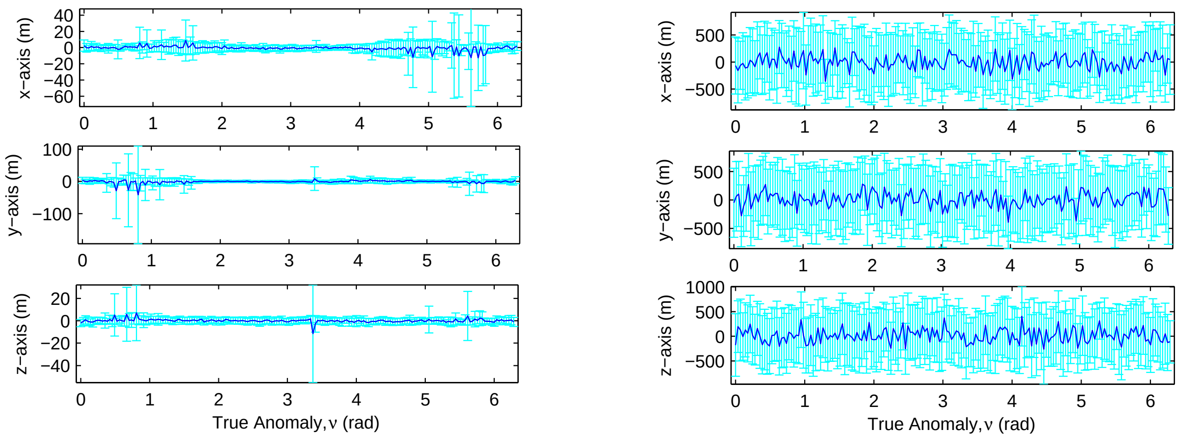

(a) With measurement errors of ±5 m, ±0.003°. (b) With measurement errors of ±1 km, ±0.01°.

Fig. 10. Mean and standard deviation (error bars) of estimated centres relative to the actual centre of Apophis.

Measurement errors were introduced on the position estimate of the spacecraft in inertial space, and the attitude determination of each spacecraft. To compensate for these errors, plus those introduced by rasterisation, the intersection points were calculated for each pair of spacecraft. A 5 spacecraft funnel formation was used, giving 20 estimated values for the centre of the NEO in inertial space. Fig. 10 shows the mean and standard deviation of a set of estimated centres relative to the actual centre of Apophis in the heliocentric inertial reference frame, over one full orbit. The camera was assumed to have a CCD array of 1768 × 1768 pixels, a total field of view of 10° and a focal length of 2.5 mm. As seen from the figures, the method shown for the navigation works in principle provided that the position of the satellites is known with good accuracy. Although an accuracy of 1 km in position has to be expected for a single spacecraft in deep space, a formation can improve this accuracy by combining the intersatellite position measurements with the position measurement based on other navigation approaches. The use of intersatellite measurements, in fact, would filter out all position errors with opposite sign. A substantial improvement in the estimation of the position of the spacecraft was theoretically proven for the mission LISA in a recent study [9]. Note that the estimated relative position of the asteroid with respect to the satellites has a much lower error due to the higher precision of the intersatellite position.

SYSTEM BUDGET

In order to assess the dry mass for a single mirror bee, a range of technology levels have been assumed from existing flight hardware (e.g. Inflatable Antenna Experiment) through to a conceptual membrane system with embedded sensing and actuation. The key driver for the mirror bee mass budget is the areal density of the adaptive reflector assembly (see Tables 1–2). It will be assumed that the reflector mass includes all associated control hardware. The spacecraft bus is assumed to be comparable to the NEAR spacecraft and is representative of a mid-sized bus operating in deep space at a solar distance of up to 2.2 AU. The NEAR dry mass is 487 kg, therefore a 500 kg bus is assumed with a 10% mass margin given the flight heritage of the NEAR spacecraft. The bus is assumed to provide power, telecommunications and attitude sensing functions. In addition to the adaptive reflector and bus, with appropriate mass margins, a system contingency of 20% is added to provide margin for integration of the bus and adaptive reflector. From previous studies [3][5] we could see that a rendezvous with Apophis with a low thrust transfer could take about 470 days, with a maximum thrust level of 0.6 N for a 3000 kg spacecraft and an I_{sp} of 3200 s. For these types of transfers, we have a non-optimised propellant consumption of 30% of the initial mass. We maintain the same assumption in this estimation of the total mass of the spacecraft. Therefore, the mass has to be augmented by a factor of 1.4 (including tanks) due to the transfer cost. The orbit control in the case of the AEP solution is negligible and could be performed with FEEP engines ($I_{sp} \approx 10000$ s) with a negligible mass consumption compared to the transfer.

Table 1. Adaptive primary mirror with 0.5 kg/m^2 areal density.

Item	TRL	Area (m^2)	Mass (kg)	Margin (%)	Total (kg)
Reflector	4	3000	1500	15	1725
Bus	9		500	10	550
Contingency				20	455
Dry Mass					2730

Table 2. Adaptive primary mirror with 0.05 kg/m^2 areal density.

Item	TRL	Area (m^2)	Mass (kg)	Margin (%)	Total (kg)
Reflector	2	3000	150	20	180
Bus	9		500	10	550
Contingency				20	146
Dry Mass					876

Table 3. Fixed primary mirror plus laser.

Component	Specific mass	Mass (kg)	Margin (%)	Subtotal (kg)	Accumulative (kg)
Primary mirror	0.05 kg/m^2	15.71	25	19.63	19.63
Directional mirror	0.1 kg/m^2	0.665	25	0.813	20.44
Laser	0.005 W/m^2	601.24	50	901.86	922.30
Solar arrays	1 kg/m^2	3.15	15	3.611	925.91
Cables	0.2 m_{elec}	185.18	0	185.18	1111.09
Radiator (solar array)	1.4 kg/m^2	420.0	20	504.0	1615.09
Radiator (laser)	1.4 kg/m^2	112.0	20	134.4	1749.49
Radiator of reflective mirror	1.4 kg/m^2	9.79	20	11.76	1761.25
Bus	-	500	20	600	2361.25
Propellant	0.4 m_{dry}	944.51	0	944.51	3305.76
Tanks	0.1 m_{fuel}	94.51	0	94.51	**3400.27**

If a laser system is used instead of the direct imaging, the spacecraft is more complex and requires more elements. Table 3 shows the mass budget for a primary parabolic (or spherical) solar collector, solar arrays to convert the solar energy into electric power, a semiconductor laser as beaming system, and cooling system for solar arrays and laser. The mass of the bus and of the primary mirror are based on the previous estimation for the direct imaging system. The laser mass accounts for the mass of the semiconductor and the cavity but no optics. We use however a margin of 50% to include the mass of the casing and optical elements. The assumption here is that the laser can operate between 0^{o}C and 40^{o}C while the solar array cannot operate above 100^{o}C. Assuming the efficiency of the laser can go up to 75%, the largest part of the power needs to be dissipated at the first stage since we do not expect an efficiency of the solar arrays higher than 40%. For this mass budget, we assumed a reference case of a solar collector with a surface area of 314 m^2 collecting 429.5 kW of power at 1 AU and a surface area of the array also of 3.14 m^2. If the solar array is operating at 40% efficiency, the cooling system will have to dissipate 2.57 MW at the first stage. The radiator, laser and solar arrays are located in the shadow of the primary mirror. A secondary reflective mirror reflects the concentrated light through a hole in the primary mirror to the back of the primary. The solar array and the laser are directly connected to the radiator. If we assume a reflectivity of the secondary mirror of 99% we would need an additional radiator attached to the secondary with a total area of 7 m^2 (assuming an absorptivity of 0.2).

CONCLUSION

In this paper we presented two possible solutions to place the mirrors in close proximity to the asteroid but out of the debrus plume. The analysis performed in this study showed that both the direct imaging concept and the laser concept appear feasible. From the computation of the mass budget for the direct imaging system, a swarm of 5-6 satellites, each carrying a 60 m diameter mirror at TRL 4, would deflect Apophis by 5e5 km with 4 years of warning time and a mass at launch of each spacecraft between 3.5 and 4.5 tons. A more reasonable swarm would need a lighter adaptive mirror, which at present appears to be at TRL 2.

A system based on a solar pumped laser with a primary mirror of smaller size (20 m in diameter) would have a comparable mass per spacecraft with the same number of spacecraft. It should be noted that for both the direct imaging and laser systems, the mass is directly proportional to the surface area and therefore proportional to the square of the aperture size of the collector. This would suggest in both cases to go for many spacecraft of small size, rather than a single large one. Furthermore, multiple superimposed beams provide a higher thrust than an equivalent increase in the concentration factor of a single beam, allowing the satellites can be placed at longer distances. The TRL of the laser solution strongly depends on the TRL of the laser and of the solar arrays. Most of the assumptions are based on current laboratory tests in both areas (which means TRL 4 or higher) but the overall system for space applications has still to be developed (TRL 2-4). The investment in the development of highly efficient lasers and solar arrays goes beyond the deflection of asteroids and is progressing very fast due to the thousands of commercial applications.

ACKNOWLEDGEMENTS

This research is partially supported by the ESA/Ariadna Study Grant AO/1-5387/07/NL/CB.

REFERENCES

[1] H. J. Melosh and I. V. Nemchinov, “Solar asteroid deviation”, *Nature*, vol. 366, pp. 21-22, 1993.

[2] R. Kahle, E. Kührt, G. Hahn and J. Knollenberg, “Physical limits of solar collectors in deflecting Earth-threatening asteroids”, *Aerospace Science and Technology*, vol. 10, pp. 253-263, 2006.

[3] J. P. Sanchez, C. Colombo, M. Vasile and G. Radice, “Multi-criteria comparison among several mitigation strategies for dangerous Near Earth Objects”, *Journal of Guidance, Control and Dynamics*, vol. 32, no. 1, pp. 121-142, 2009.

[4] J. P. Sanchez, M. Vasile and G. Radice, “On the consequences of a fragmentation due to a NEO mitigation strategy”, *International Astronautical Congress*, IAC-08-C1.3.10, Glasgow UK, 2008.

[5] C. Colombo, M. Vasile, and G. Radice, “Semi-analytical solution for the optimal low-thrust deflection of Near-Earth Objects”, *Journal of Guidance, Control and Dynamics*, in press, 2009.

[6] M Vasile, C Maddock and G Radice, “Mirror Formation Control in the Vicinity of an Asteroid”, *AAS Astrodynamics Specialist Conference and Exhibit*, AIAA 2008-6252, Honolulu, Hawaii, 2008.

[7] M. Vasile, “A multi-mirror solution for the deflection of dangerous NEOs”, *Communications in Nonlinear Science and Numerical Simulation*, DOI 10.1016, 2008.

[8] H. Schaub, J. L. Junkins, *Analytical mechanics of space systems*, AIAA Education Series, Virginia USA, 2003.

[9] C. Maddock and M. Vasile, “Design of optimal spacecraft-asteroid formations through a hybrid global optimization approach”, *Journal of Intelligent Computing and Cybernetics*, vol. 1, no. 2, pp. 239-268, 2008.

[10] L. R. Chung, “Orbit Determination Methods for Deep Space Drag-Free Controlled Laser Interferometry Missions”, M.Sc. Thesis, University of Maryland USA, May 2006.